

Deformation Mechanisms at Elevated Temperatures: Influence of Momenta and Energy in the Single Impact Test

Harald Rojacz, Markus Varga, and Horst Winkelmann

Abstract—Within this work High Temperature Single Impact Studies were performed to evaluate deformation mechanisms at different energy and momentum levels. To show the influence of different microstructures and hardness levels and their response to single impacts four different materials were tested at various temperatures up to 700°C. One carbide reinforced NiCrBSi based Metal Matrix Composite and three different steels were tested. The aim of this work is to determine critical energies for fracture appearance and the materials response at different energy and momenta levels. Critical impact loadings were examined at elevated temperatures to limit operating conditions in impact dominated regimes at elevated temperatures. The investigations on the mechanisms were performed using different means of microscopy at the surface and in metallographic cross sections. Results indicate temperature dependence of the occurrence of cracks in hardphase rich materials, such as Metal Matrix Composites High Speed Steels and the influence of different impact momenta at constant energies on the deformation of different steels.

Keywords—Deformation, High Temperature, Metal Matrix Composite, Single Impact Test, Steel.

I. INTRODUCTION

THE understanding of different deformation mechanisms at all temperature stages is crucial for the optimal use of materials. Single impact loadings often lead to materials failure, especially in high temperature environment [1]. To reveal the optimal field of application, it is of great importance to understand the correlation of the materials microstructure, the resulting hardness and their change at increasing temperature [2]-[4]. It is well known that materials microstructure and further its behavior in different loading regimes can be changed by heat treatment [5]. As seen in numerous literatures martensitic steels reveal high hardness at comparatively good ductility [6]-[8]. With an increased amount of hardphases the ductility of materials decreases and outbursts or materials collapse occur [9], [10]. Also the loading condition has a crucial influence on the deformation behavior. It is well known that the time span of the deformation is of great significance [11]. Lower momenta causes less ductile behavior and can lead to a change in the

deformation mechanism—elasto-plastic dominated deformation can switch to pure plastic deformation; cracks and outbursts are formed. Also the temperature highly affects the deformation behavior of materials.

Due to thermal effects materials soften and microstructural changes occur [12], [13]. Especially break outs my increase If secondary precipitations are present [14]. Even high temperature resistant materials such as metal matrix composites (MMC) and high speed steels (HSS) loose their excellent high temperature properties, like wear and oxidation resistance exceeding a certain temperature [15], [16]. In this work single impact studies were performed to show different influences on the deformation behavior. (i) The influence of the heat treatment should be shown, by a carbon steel in two different heat treatment conditions; normalised and annealed martensitic. (ii) Two annealed steels, a carbon steel and a hot work tool steel with martensitic structure was chosen for comparative investigation. (iii) The influence of hardphases one high speed steel with 25% hardphases and one TiC-NiMo particle reinforced NiCrBSi based MMC (40% hardphases) were chosen. Further the influence of different amounts of hardphases and their resulting deformation behavior can be investigated at these materials.

This work aims at High Temperature Single Impact (HT-SIT) studies to limit the range of application of different material classes up to 700°C. The influence of the heat treatment conditions at a constant chemical composition and the comparison of the deformation behavior of similar microstructures with different chemical compositions is investigated.

II. EXPERIMENTAL

A. Materials Data

In this work different material classes were chosen for examinations. Material A and B have the same chemical composition – a carbon steel according to AISI 1045 or 1.1191. Material A was tested in normalized condition, whereas Material B was tested in hardened and tempered condition. Material C is a hot work tool steel in annealed condition with a chemical composition according to AISI H11 or 1.2343. Material D is a powder metallurgical manufactured high speed steel (in annealed condition), revealing very high hardness and precipitated hardphases, with high amounts of Cr, Mo, W, V and Co.

H. Rojacz is with the Austrian Center of Competence for Tribology (AC²T research GmbH), Wiener Neustadt, 2700 AUT (phone: 00432622-81600-171; e-mail: rojacz@ac2t.at)

H. Winkelmann was with the Austrian Center of Competence for Tribology (AC²T research GmbH), Wiener Neustadt, 2700 AUT.

Material E is a NiCrBSi-based hardfacing reinforced with 40% of TiC-NiMo hardphases in an optimized Plasma Transferred Arc (PTA) cladding process using an EuTronic® Gap 3001 DC apparatus with optimized welding parameters by Zikin et al. [6], [9], [16]. The chemical compositions of all materials investigated are given in Table I. To reveal the microstructure, metallographic samples were prepared with subsequent grinding, polishing and subsequent etching. Materials A-D were etched with 4 % HNO₃ in ethanolic solution for about 5 seconds. Etchant of Material E was a mixture of HF and HNO₃ in a volume ratio of 1:12 used at room temperature for 10 seconds. Microstructural examinations were performed by means of optical microscopy (OM). Chemical compositions and heat treatments of all materials investigated are given in Table I.

TABLE I
CHEMICAL COMPOSITION OF THE MATERIALS INVESTIGATED

Material	Chemical Composition	Heat Treatment
Material A	0.45% C, 0.25% Si, 0.65% Mn, Fe bal.	normalised
Material B	0.45% C, 0.25% Si, 0.65% Mn, Fe bal.	annealed
Material C	0.4% C, 1.1% Si, 0.4% Mn, 5.0% Cr, 1.3% Mo, 0.4% V, Fe bal.	annealed
Material D	2.0% C, 0.5% Si, 3.8% Cr, 2.5% Mo, 5.1% V, 14.3% W, 11.0% Co, Fe bal.	annealed
Material E	Matrix: 0.2% C, 4% Cr, 1% B, 2.5% Si, 2% Fe, 1% Al, rest Ni. Hardphase: 80% TiC, 20% Ni:Mo 2:1.	none

B. Hot Hardness Data

The Hot Hardness Test (HHT) rig is based on the Vickers method (HV10) enhanced to elevated temperatures, developed at the Austrian Centre of Competence for Tribology (AC²T research GmbH). Materials hardness up to 800°C can be determined. The indents are examined by OM using a Leica MEF4A microscope with a Leica DFC 450 camera. Three indents per temperature were performed for the homogenous Materials A-C; eight indents for the Materials D and E due to the high diversity of hardness in different phases. Data of Material A and E were previously presented [6], [18].

C. High Temperature Single Impact Test (HT-SIT)

The HT-SIT, which can be seen in Fig. 1(a), was developed to investigate the high temperature impact behavior of materials. With this test rig it is possible to examine impacts at several impact energies (0.25-100 J) and momenta (1.11-44.72 Ns) in a temperature range of 20-1000°C. The test principle is based on an impact sledge with defined potential energy, which is dropped (turned to kinetic energy by free fall – Fig. 1(b), which leaves a defined wear mark.

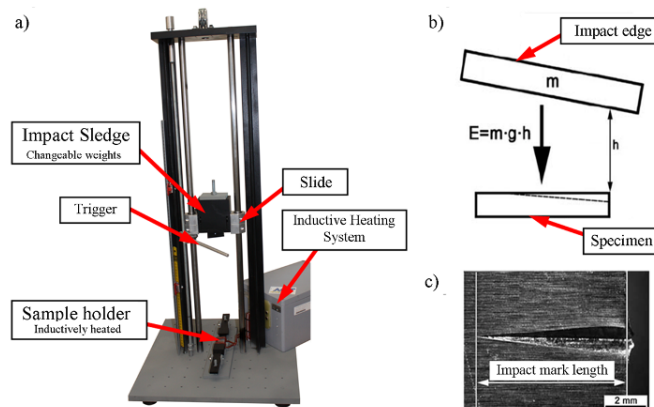


Fig. 1 High Temperature Single Impact Test Rig: (a) Overview, (b) Test principle, (c) Measuring of the impact mark length.

TABLE II
TEST PARAMETERS FOR ENERGY AND MOMENTUM SENSITIVE MEASUREMENTS

Temperature [°C]	20, 300, 500, 700
Energy [J]	1, 2, 4, 8
Momentum [Ns]	3.13, 4.43, 6.26

The impact sledge consists of a dropping head with changeable weights hauled by a horizontally arranged impact edge with an angle of 5°. Parameters are defined by the potential energy $E_{pot} = m \cdot a \cdot s$ and a momentum $p = m \cdot v$, where m is the mass, a the gravitational acceleration, s the initial height (so the dropping distance) and v the velocity. For this series of experiments the energy was set and the momentum was defined. After the impact sledge hits the sample with defined parameters, temperature, energy and momentum the impact length can be measured in Fig. 1(c), which gives a correlation of three parameters on the deformation. This is done by means of OM and gives an overview on the deformation behavior at a first shot. If there are no cracks or outbursts, the impact length can be measured valid. Parameters for the energy and momentum sensitive measurements are given in Table II.

TABLE III
TEST PARAMETERS FOR DETERMINING CRITICAL ENERGIES

Temperature [°C]	20, 350, 550, 700
Energy [J]	0.25, 0.5, 0.75, 1, 1.5, 2, 2.5, 3, 3.5, 4, 6, 8
Drop weight [kg]	3.13, 4.43, 6.26

If there are cracks, it has to be determined if the energy is subcritical or critical, however the deformation behavior has switched from elasto-plastic to plastic. The subcritical energy $E_{subcrit}$ was defined as the energy where cracks start to form.

Once failures become significant, which means cracks running down the substrate of the coating, outbursts or displacement of a coating against the substrate occurs, the impact energy can be considered critical for the material (E_{crit}). The energy beyond which these failures occur is critical. Burden impact loads should not exceed this energy in applications. Failure and decay of machine parts can occur

exceeding this energy. For bulk materials, this happens if deep cracks or massive material deflection occur. A more detailed description can be found in previous studies of Rojacz et al. [6]. Further shall be mentioned, that also the critical energy is a function of momentum and temperature $E_{crit}(p,T)$. Parameters for determining critical energies are given in Table III.

For ductile Materials A-C the studies were focused on the deformation behavior at different energy and momenta levels at ambient and elevated temperatures. For Material D and E the focus was set on the examination of critical materials behavior, limiting the range of operation in impact dominated systems, due to brittle materials behavior influenced by hard phases. For a detailed understanding scanning electron microscopy (SEM) with a Zeiss Supra 40 VP was performed and metallographic cross sections were prepared for microstructural examinations.

NiCrBSi matrix. The compound hardness of this hardfacings is about $650 \text{ HV}_{10} \pm 24 \text{ HV}_{10}$ at room temperature.

B. Hot Hardness Data

The Hot Hardness data of all materials are given in Fig. 3.

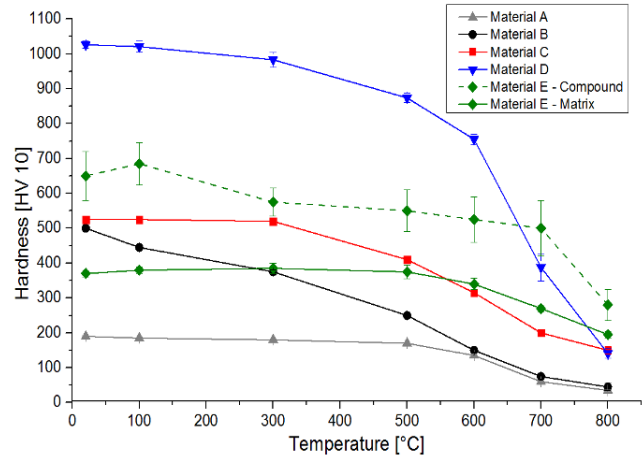


Fig. 3 Temperature-Hardness-Curves of all materials investigated

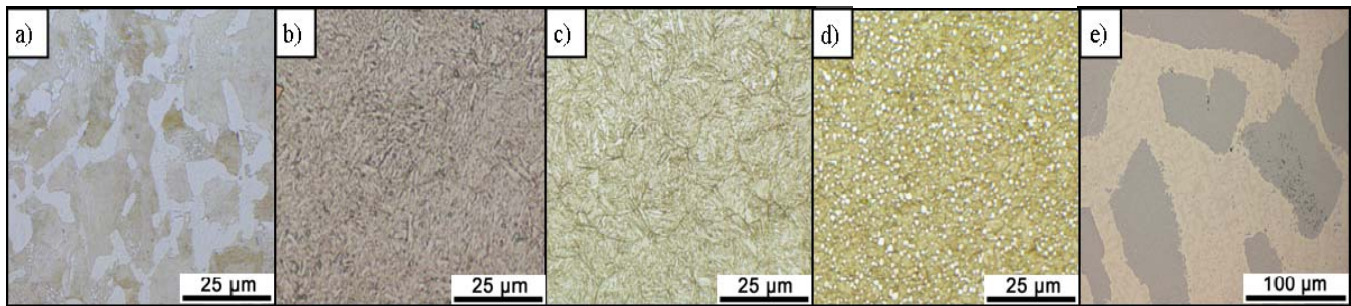


Fig. 2 Overview on the microstructural analysis: (a) Material A, (b) Material B, (c) Material C, (d) Material D, (e) Material E

III. RESULTS AND DISCUSSION

A. Microstructural Analysis

An overview on the microstructural analyses, done with OM, is given in Fig. 2. Material A and B are a carbon steel in different heat treatment condition. Material A, as seen in Fig. 2a is in normalised condition revealing ferritic-pearlitic microstructure and a hardness of $190 \pm 2 \text{ HV}_{10}$. Material B (annealed condition) shows annealed martensitic structure with a hardness of $498 \pm 4 \text{ HV}_{10}$. The microstructure can be seen in Fig. 2b. Material C is a hot work tool steel, depicting martensitic microstructure (Fig. 2c) and a hardness of $525 \pm 3 \text{ HV}_{10}$. Material D is a powder metallurgical high speed steel with high amounts of alloying elements like Cr, Mo, V and W in oil hardened condition resulting in a hardness of $1026 \pm 10 \text{ HV}_{10}$ and annealed martensitic structure with 20-25 % homogenously distributed fine primary carbides, as seen in Fig. 2d. Material E (as seen in Fig. 2e) is a NiCrBSi-based, PTA-welded hardfacings with 40 wt-% TiC-NiMo hardphases as a reinforcement. A more detailed description of this hardfacing was done by Zikin et al. [17], [18]. As seen in Fig. 2e Material E show TiC-NiMo hardphases embedded in a

The data of Materials A and E were previously presented [6], [18]. The hardness investigation at increased temperature is not the focus of this study, but it is crucial to understand softening mechanisms, because they strongly influence the impact and deformation behavior of materials. Material A slightly loses its hardness up to 500°C , dropping rapidly when exceeding this temperature. For Material B a nearly linear hardness decrease can be detected from about 500 HV_{10} to 40 HV_{10} at 800°C due to annealing effects until 700°C and further due to the different microstructure (austenitic) at 800°C . Material C shows good stability against softening up to 500°C ; Exceeding this temperature, the hardness drops to 200 HV_{10} at 800°C . Material D, the HSS shows linear hardness decrease up to 500°C . At 600°C Material D has still about 750 HV_{10} ; after 600°C the hardness drops. Material E shows constant hardness level up to 700°C due to a very stable matrix and hardphases; exceeding 700°C the matrix begins to soften.

C. Macroscopical Influences On the Deformation Behavior of Different Steels

In this section macroscopical effects of the deformation at constant energy levels and different momenta and temperatures are discussed. In Fig. 4 the impact mark length curves of Material A, B and C are given to show the influence of different momenta at constant energy levels in impact dominated systems, also at elevated temperature. Data of Material A was previous presented by Rojacz, et al [6].

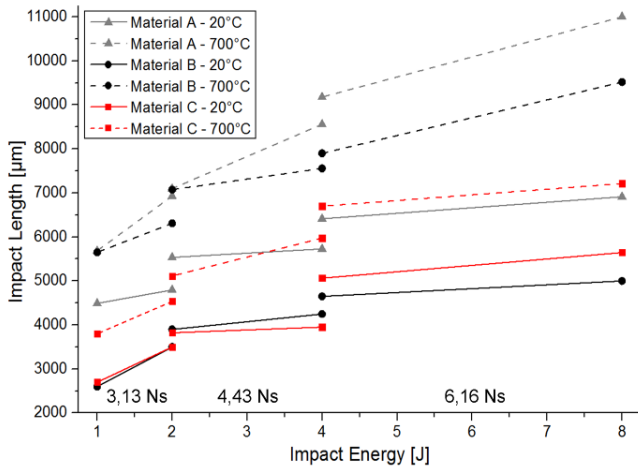


Fig. 4 Impact Energy – Impact Length correlation of Material A, B and C at different momenta at 20°C and 700°C

As seen in the figure, for all materials and temperatures there is a logarithmic coherence of energy and impact length within the energy sensitive measurements. All materials investigated show increased sensitivity of the momenta at higher energies and momenta at room temperature. Different materials behavior can be seen at elevated temperature.

D. Influence of Different Microstructures of Steels at a Given Chemical Compositions on Materials Deformation

As seen in Fig.4 the microstructure strongly affects the materials impact behavior at a given chemical composition. Harder microstructures, such as martensitic phases (Material B) reveal less deformation than softer ones, such as the normalized state (ferritic-pearlitic steel) Material A. At constant chemical composition, the hardness is primarily resulting from the heat treatment and the microstructure. In general, based on these findings can be said, that higher hardness at the same composition results in less deformation. Elasto-plastic deformation is the main deformation mechanism in these materials.

For the high temperature deformation behavior different influences can be seen. At 700°C the both materials show nearly the same low hardness (see section III B Hot Hardness Data). The difference in the impact lengths at 700°C can be ascribed to differences in the microstructures. In Material A, the pearlite forms spherical soft annealed pearlite exceeding 550°C which decreases the hardness rapidly. Martensitic Material B softens due to annealing processes. For elevated temperatures the hardness strongly is influenced by thermal processes, such as annealing and phase transformation. For the

same chemical composition the influence of the initial microstructure becomes more and more negligible at elevated temperatures. When exceeding a phase transformation temperature (in this case the eutectoidal line at 723°C in the Fe-Fe₃C-phase diagram) the deflection of both initial conditions will be similar; in our case, the martensite shows better resistance against impacts; also Material B gets less sensitive to higher momenta with increasing temperature and energy, while Material A reveals higher sensitivity to increased momenta, due to fine dispersed Fe₃C hardphases (soft annealed pearlite).

E. Influence of Defined Hardness and Microstructure with Different Chemical Compositions

For the comparison of materials at the similar microstructure (also similar hardness) but different chemical compositions Material B and C were chosen. Their annealed martensitic microstructure reveals excellent impact resistance at a good ductility. No cracks or outbursts can be found at these materials. As seen in Fig. 4 Material C, due to higher amounts of other alloying element than Material B, shows higher influence of the momenta at higher energies. This is mainly influenced by the different hardening mechanisms. While Material B raises its hardness only by the formation of martensite due to quenching in water and further annealing; Material C on the other hand has two hardening effects: the formation of martensite and solid solution strengthening due to alloying elements such as Mn, Cr, V and Mo [19].

Martensitic materials (Material B and C) show different behavior at elevated temperature. Due to the high amounts of temperature resistance increasing alloying elements in Material C, higher hardness leads to smaller impacts at 700°C. Material C, in fact is a hot work tool steel, which entails good impact resistance up to 700 °C. The ductile behavior can be ascribed to the lack of hardphases; the good impact resistance can be affiliated to the high stability against softening processes up to 700 °C. High momentum sensitivity can be seen in the Impact Energy – Impact mark length diagrams due to the alloying elements, stabilizing against annealing processes at 700 °C.

F. Fracture Behavior of Hardphase Rich Materials at Elevated Temperatures

To show plastic deformation mechanisms at elevated temperatures, one hardphase rich HSS (Material D) and one TiC-NiMo particle reinforced MMC (Material E) were tested regarding their cracking behavior at different impact energies. Critical energies E_{crit} and $E_{subcrit}$ of Material D and E and their temperature dependence can be seen in Fig. 5.

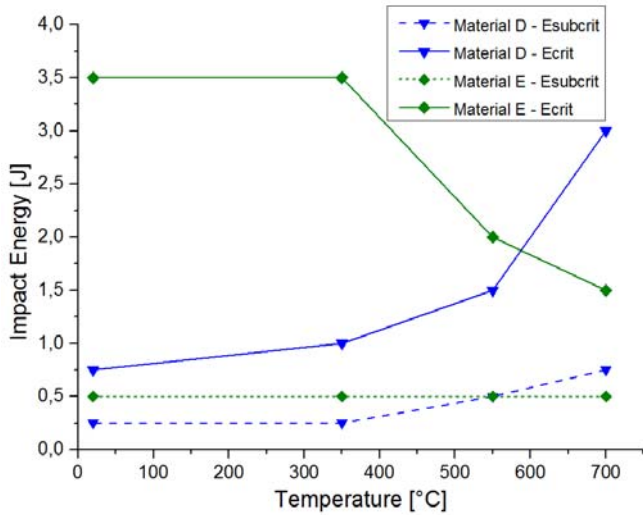


Fig. 5 Temperature dependency of critical materials behavior in the Single Impact Test

Material D shows highly critical behavior. Due to the fine dispersed hardphases and the high initial hardness (~1000 HV10) first fractures occur at 0.25 J; critical cracks and outbursts occur at 0.75 J at room temperature. With increasing temperatures softening mechanisms occur. The martensitic matrix starts to anneal, while the carbides (tungsten, vanadium, cobalt and molybdenum carbides) don't show any softening effects; so the subcritical energy E_{subcrit} rises up to 0.75 at 700°C. Even stronger temperature dependence can be seen for the critical energy E_{crit} . Due to the matrix softening at elevated temperature the mechanical backup decreases, but a critical crack can be stopped in this softened matrix [3]. The critical energy is raised up to 1.5 J at 500°C; exceeding 600°C the hardness of Material D drops and even less critical behavior (3 J) at 700°C can be seen. SEM-Images of the surface and metallographic cross sections of typical subcritical and critical behavior of Material D can be seen in Fig. 6. This decrease of the critical behavior can be affiliated to the high quantity of the hardphases, but their small size (~1-2 μm) and their homogenous distribution (powder metallurgical manufactured). This decrease of the critical behavior can be affiliated to the high quantity of the hardphases, but their small size (~1-2 μm) and their homogenous distribution (due to powder metallurgical manufacturing). As seen in Fig. 6(a) and Fig. 6(c) the subcritical energy can not be detected by surface analysis. Cracks occur under the surface, which can be pointed out as undercritical for corrosion or increased attack by cyclic impact (and also combined abrasive) wear [2]-[4], [19].

For critical behavior huge decay of Material D occurs (Fig. 6(b) and (d)); outbursts and brittle materials behavior can be seen.

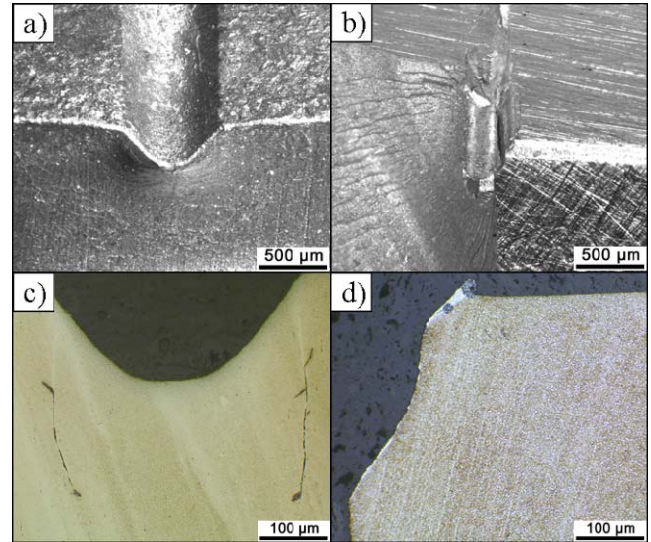


Fig. 6 Overview on typical critical impact energies of Material D: (a) SEM surface image of E_{subcrit} , (b) SEM surface image of E_{crit} , (c) Cross section of E_{subcrit} by means of OM, (d) Cross section of E_{crit} by means of OM

For Material E different materials behavior can be detected. The subcritical energy shows no dependence to temperature dependence in the tested temperature array. E_{subcrit} is 0.5 J. Subcritical behavior can be detected below 3.5 J up to 350°C; decreasing at higher temperatures (as seen in Fig. 5). Critical behavior strongly depends on the tested temperature. Typical subcritical and critical impact marks and their cross sections are given in Fig. 7.

At subcritical impact energies stable cracking is the main deformation behavior at all tested temperatures due to comparatively big hardphases (100 μm) and the high distance between them. The cracks are formed through prior phases due to the small bonding interface of matrix and carbide. Carbide fracture occurs in a small amount. At elevated temperature the same mechanisms can be detected for subcritical impacts. At critical impact energies above 3.5 J up to 350°C mechanisms change. Unstable cracks are formed; carbide fracture is present at all tested temperatures.

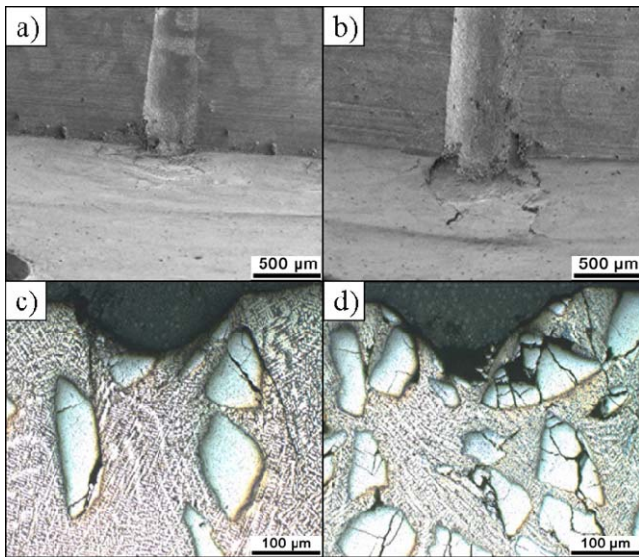


Fig. 7 Overview on typical critical impact energies of Material E:
 a) SEM surface image of E_{subcrit} , b) SEM surface image of E_{crit} ,
 c) Cross section of E_{subcrit} by means of OM, d) Cross section of E_{crit}
 by means of OM

This cracking can be affiliated to the higher brought in fracture energy. These effects are caused by the missing mechanical backup of the matrix and the high diversity of hardness [20] and gets even more present at elevated temperatures. In the presence of hardphases subcritical impact energies, which cause first, undercritical cracks are at a very low energy. These subcritical energies do not, or do marginally depend on the temperature. Critical impact energies are strongly temperature dependent [6], [21]. On the one hand a High Speed Steel with small ($<5 \mu\text{m}$) and homogenously distributed hardphases, concomitant with high hardness leads to low critical energies. Brittle materials behavior occurs at room temperature, but with increasing temperature, matrix softening occurs - less critical behavior can be detected. On the other hand, hardfacings with comparatively big ($\sim 100 \mu\text{m}$) hardphases react critical at higher energies. Increasing the temperature leads to more brittle behavior due to the high hardness diversity at higher temperatures. Due to the missing matrix backup the more critical behavior occurs. For the cracking behavior of different hardphase rich materials in impact dominated systems can be said, that the decay of MMC strongly depends on the temperature and the size, the distance and the bonding between matrix and hardphases; the HSS is strongly influenced by the hardphase content, the martensite softening mechanisms and the distribution of the hardphases.

IV. CONCLUSION

Following conclusion can be drawn on the high temperature deformation mechanisms of different material classes under single impact conditions:

- Lower momentum leads to smaller deformation due to a shortened time span for the deformation process resulting

in a more brittle materials behavior.

- The deformation strongly depends on the microstructure, consequently their hardness. Ductile materials behavior can be found for carbon steels, even at harder microstructures, such as martensites, but will change with elevated temperatures. Due to softening and microstructural changes at elevated temperatures the impact behavior of steels at a given chemical compositions is different. But when phase transition occurs or the materials hardness is nearly the same again, impacts cause the same deformation.
- At a given microstructure, the deformation strongly depends on the alloying elements, especially at elevated temperatures which can reduce materials softening and annealing effects.
- Critical materials behavior of hardphase rich materials is strongly dependent on the hardphase size, their content in a matrix, and their distribution. For elevated temperatures materials softening of the matrix and the high hardness diversity can switch properties.

ACKNOWLEDGMENT

This work was funded by the “Austrian Comet-Program” (governmental funding program for pre-competitive research) via the Austrian Research Promotion Agency (FFG) and the TecNet Capital GmbH (Province of Lower Austria) and has been carried out within the “Austrian Center of Competence for Tribology” (AC²T Research GmbH). Authors are grateful to voestalpine Stahl GmbH for active research cooperation.

REFERENCES

- [1] J.A. Collins, H. Busby, G.H. Staab, *Mechanical Design of Machine Elements and Machines*. Hoboken: Wiley VCH, 2003, ch.4.
- [2] H. Winkelmann, E. Badisch, M. Kirchgäßner, H. Danninger, “Wear Mechanisms at High Temperatures. Part 1: Wear Mechanisms of Different Fe-Based Alloys at elevated temperatures,” *Tribol. Letters*, vol. 34, pp. 155-166, March 2009.
- [3] H. Winkelmann, M. Varga, E. Badisch, H. Danninger, “Wear Mechanisms at High Temperatures. Part 2: Temperature Effect on Wear Mechanisms in the Erosion Test,” *Tribol. Letters*, vol. 34, pp. 167-175, March 2009.
- [4] H. Winkelmann, E. Badisch, M. Varga, H. Danninger, “Wear Mechanisms at High Temperatures. Part 3: Changes of the Wear Mechanisms in the Erosion Test,” *Tribol. Letters*, vol. 37, pp. 419-429, January 2010.
- [5] H.J. Bargel, G. Schulze, *Werkstoffkunde*. Heidelberg: Springer-Verlag, 2008, ch.1.
- [6] H. Rojacz, M. Hutterer, H. Winkelmann, “High temperature single impact studies on material deformation and fracture behavior of metal matrix composites and steels,” *Materials Sci. and Eng. A*, vol. 562, pp. 39-45, November 2012.
- [7] S. Tianmin, H. Meng, T.H. Yuen, “Impact wear behavior of laser hardened hypoeutectoid 2Cr13 martensite stainless steel,” *Wear*, vol. 255, pp. 444-455, August 2003.
- [8] H. Rojacz, H. Winkelmann, M. Varga, “Verhalten von Eisenbasiswerkstoffen unter Einzelschlagbelastung,” in Proc. ÖTG Symposia 2011, Wiener Neustadt, 2011, pp- 143-152.
- [9] A. Zikin, I. Hussainova, C. Katsich, E. Badisch, C. Tomastik, “Advanced chromium carbide-based hardfacings,” *Surface and Coatings Technol.*, vol. 206, pp. 4270-4278, May 2012.
- [10] M. Kirchgäßner, E. Badisch, F. Franek, “Behavior of iron-based hardfacing alloys under abrasion and impact,” *Wear*, vol. 265, pp. 772-779, August 2006.

- [11] K. Wellinger, H. Breckel, "Kenngrossen und Verschleiss beim Stoss metallischer Werkstoffe," *Wear*, vol. 13, pp. 257-281, April 1969.
- [12] E. Hornbogen, G. Eggeler, E. Werner, *Werkstoffe - Aufbau und Eigenschaften*. Heidelberg: Springer-Verlag, 2012, ch.4.
- [13] S.L. Kakani, A. Kakani, *Materials Science*, New Delhi: New Age Publishers, 2004, ch.7.
- [14] H. Winkelmann, M. Varga, E. Badisch, "Influence of Secondary precipitation in Fe-based MMCs on high temperature wear," *Tribol. Letters*, vol. 43, pp.229-235, Aug. 2011.
- [15] N. Chawla, K.K. Chawla, *Metal Matrix Composites*, New York: Springer, 2000, ch.10.
- [16] H. Rojacz, A. Zikin, C. Mozelt, H. Winkelmann, E. Badisch, "High temperature corrosion studies of cermet particle reinforced NiCrBSi hardfacings," *Surface and Coatings Technol.*, vol. 222, pp. 90-96, February 2013.
- [17] A. Zikin, E. Badisch, I. Hussainova, C. Tomastik, H. Danninger, "Characterisation of TiC-NiMo reinforced Ni-based hardfacing," *Surface and Coatings Technol.*, to be published.
- [18] A. Zikin, M. Antonov, I. Hussainova, L. Katona, A. Gavrilovic, "High temperature wear of cermet particle reinforced NiCrBSi hardfacings," *Tribology Int.*, to be published.
- [19] G. Krauss, "Martensite in steel: strength and structure," *Mater. Sci. and Eng.*, vol. A 273, pp. 40-57, Dec. 1999.
- [20] G. W. Stachowiak, A.W. Batchelor, *Engineering Tribology*. Burlington: Elsevier Butterworth Heinemann, 2005, ch. 15.
- [21] R.O. Ritchie, "Mechanisms of fatigue-crack propagation in ductile and brittle solids," *Int. J. of Fracture*, vol. 100, pp. 55-83, May 2008.